Central European Science Journals
w w w . c e s j . c o m

Central European Journal of Physics
Central European Science Journals
CEJP 3(2) 2005 303–323

Solutions of the Schrödinger equation for Dirac delta decorated linear potential

Haydar Uncu[1*], Hakan Erkol[1†], Ersan Demiralp[1,2‡], Haluk Beker[1§]

[1] *Physics Department,*
Boğazici University,
Bebek, 34342, Istanbul, Turkey

[2] *Boğazici University-TÜBITAK Feza Gürsey Institute,*
Kandilli, 81220, Istanbul, Turkey

Received 21 October 2004; accepted 21 February 2005

Abstract: We have studied bound states of the Schrödinger equation for a linear potential together with any finite number (P) of Dirac delta functions. For $x \geq 0$, the potential is given as

$$V(x) = f\,x - \frac{\hbar^2}{2m}\sum_{i=1}^{P}\sigma_i\,\delta\left(x - x_i\right)$$

where $0 < f$; $0 < x_1 < x_2 < \ldots < x_P$, the σ_i are arbitrary real numbers, and the potential is infinite for $x < 0$.
© Central European Science Journals. All rights reserved.

Keywords: Bound State, linear potential, Dirac delta functions
PACS (2000): 03.65.Ge

1 Introduction

The linear potential $V = f\,r$ is commonly utilized to describe confined particles since it tends to infinity as $r \to \infty$. The charmonium is a good example of such a system and it is successfully described by means of a linear potential [1]. Linear potentials are also used to model systems in solid state physics [2], high energy physics and statistical physics [3, 4]. The Schrödinger equation with linear potential is exactly solvable [5].

* E-mail: uncu@boun.edu.tr
† E-mail: hakanerkol78@hotmail.com
‡ E-mail: demirale@boun.edu.tr
§ E-mail: bekerh@boun.edu.tr

Dirac delta potentials are very useful to model contact or very short range interactions [6]. The Kronig-Penney model, contact interactions of some particles with ring shaped polymeric molecules, and carbon nanotubes are some of the physical systems which may be modelled by using Dirac delta potentials [7, 8, 9]. Additionally, Uchino and Tzutsi used Dirac delta potentials in their interesting study on supersymmetry in quantum mechanics [10].

The aim of this paper is to introduce the Dirac delta decorated linear potential and solve it for the most general case. It may be useful to consider this potential to model systems that have very short range interactions in addition to a linear potential. Extremely narrow one-dimensional quantum wells, such as layered GaAs/GaAlAs structures, can be synthesized [11]. Bound states of a charged particle in the presence of an external constant electric field in multiple ultrathin quantum wells (or impurities) can be investigated by using our model, using Dirac delta functions to describe the ultrathin quantum wells (or impurities). Particle scattering and photoionization problems related to such systems can be studied by introducing Dirac delta potentials [12, 13]. A potential which is created by charge transfers at junctions of heterostructures such as GaAs/GaAlAs can be approximately modelled using a linear potential. These types of quantum wells are called triangular quantum wells [14]. Very short-range impurity effects on top of this linear potential in a triangular quantum well can be investigated by using Dirac delta functions.

In Section 2, we present solutions of the one-dimensional Schrödinger equation with Dirac delta decorated linear potential. We first find transfer matrices and then the total transfer matrix, which is necessary to determine an energy eigenvalue equation using the method described in [7]. We obtain the ground state energy numerically for P=1, 2, 4, 8 cases with attractive and repulsive Dirac delta potentials. For P=1, we calculate the eigenvalue equation explicitly and check the limit where σ, the strength of the Dirac delta potential, goes to zero to obtain the well-known eigenvalue equation for the linear potential [5]. We also investigate the change in ground state energy for a potential with Dirac delta functions at random locations.

2 Results and Discussions

We first obtain the wavefunctions of the Schrödinger equation

$$-\frac{\hbar^2}{2m}\frac{d^2\Psi(x)}{dx^2}+V(x)\,\Psi(x)=E\,\Psi(x) \tag{1}$$

where, for $x \geq 0$, the potential is given as

$$V(x)=f\,x-\frac{\hbar^2}{2m}\sum_{i=1}^{P}\sigma_i\,\delta(x-x_i) \tag{2}$$

and the potential is infinite for $x < 0$. Here, the positions of the Dirac delta functions x_i are positive and the σ_i are arbitrary real numbers (where a positive σ_i represents an

attractive potential while a negative σ_i represents a repulsive one). We take the strengths of the Dirac delta functions as $\left(-\frac{\hbar^2}{2m}\sigma_i\right)$ for computational convenience. Introducing $E=\frac{\hbar^2k^2}{2m}$, we obtain from Equation (1)

$$\frac{d^2\Psi\left(x\right)}{dx^2}-\left(\frac{2mfx}{\hbar^2}-\sum_{i=1}^{P}\sigma_i\delta(x-x_i)-k^2\right)\Psi\left(x\right)=0\ . \tag{3}$$

We denote $(0,x_1)$ as the first interval, (x_i,x_{i+1}) for $i=1,...,P-1$ as the $(i+1)^{th}$, and (x_P,∞) as the $(P+1)^{th}$. Defining

$$l=\left(\frac{\hbar^2}{2mf}\right)^{\frac{1}{3}}\ and\ u=\frac{x}{l}-k^2\,l^2\ , \tag{4}$$

Equation (3) becomes

$$\frac{d^2\Psi\left(u\right)}{du^2}-\left(u-l\sum_{i=1}^{P}\sigma_i\delta(u-u_i)\right)\Psi=0 \tag{5}$$

where $u_i=\frac{x_i}{l}-k^2\,l^2$. This equation reduces to an Airy differential equation for $u\neq u_i$. The solutions of this differential equation are the Airy functions $Ai\left(u\right)$ and $Bi\left(u\right)$. The boundary conditions at $x=0\,(u=-k^2l^2)$ and $x=\infty\,(u=\infty)$ force us to choose

$$\Psi\left(-k^2l^2\right)=0\ ,\ \ \Psi\left(\infty\right)=0\ . \tag{6}$$

We define $\Psi_A=Ai\left(u\right)$ and $\Psi_B=Ai\left(u\right)-\lambda\,Bi\left(u\right)$ where $\lambda=\frac{Ai\left(-k^2\,l^2\right)}{Bi(-k^2\,l^2)}$ as the functions which satisfy the boundary conditions at $x=\infty$ and $x=0$, respectively. Hence, the wave function for the first (leftmost) interval is

$$\Psi_1=b_1\Psi_B\left(u\right)=b_1\left(Ai\left(u\right)-\lambda\,Bi\left(u\right)\right) \tag{7}$$

where b_1 is a constant. By varying the σ_i, $Bi\left(-k^2\,l^2\right)$ may become zero with λ going to infinity. However, we first consider $Bi\left(-k^2\,l^2\right)\neq 0$ and then study the cases $Bi\left(-k^2\,l^2\right)=0$. Similarly, by using the boundary condition at $x=\infty$

$$\Psi_{P+1}=a_{P+1}\Psi_A\left(u\right)=a_{P+1}Ai\left(u\right) \tag{8}$$

is taken as the wavefunction of the $(P+1)^{th}$ (rightmost) interval since $Bi\left(x\right)$ [or $Bi\left(u\right)$] becomes infinite as $x\rightarrow\infty$ [or $u\rightarrow\infty$]. For the intermediate regions, we choose the wavefunctions as linear combinations of Ψ_A and Ψ_B,

$$\Psi_i\left(u\right)=a_i\ \Psi_A\left(u\right)+b_i\ \Psi_B\left(u\right) \tag{9}$$

where a_i and b_i are determined by applying the boundary conditions at the interfaces of the intervals and normalizing the wavefunction. By integrating Equation (3) from $x_i-\epsilon$ to $x_i+\epsilon$ and taking the limit $\epsilon\rightarrow 0^+$, we find that the derivative will have a finite jump at

$x = x_i$ (There is a finite difference between the derivatives at $x = x_i + \epsilon$ and $x = x_i - \epsilon$). By using the continuity of the wavefunction and the jump in its derivative, we find the matrix equation

$$\begin{bmatrix} \Psi_A & \Psi_B \\ \Psi'_A & \Psi'_B \end{bmatrix} \begin{bmatrix} a_{i+1} \\ b_{i+1} \end{bmatrix} = \begin{bmatrix} \Psi_A & \Psi_B \\ \Psi'_A - \sigma_i \Psi_A & \Psi'_B - \sigma_i \Psi_B \end{bmatrix} \begin{bmatrix} a_i \\ b_i \end{bmatrix} \tag{10}$$

where primes denote differentiation with respect to x. Solving this equation for the column vector $\begin{bmatrix} a_{i+1} \\ b_{i+1} \end{bmatrix}$, we get the recursion relation

$$\begin{bmatrix} a_{i+1} \\ b_{i+1} \end{bmatrix} = \begin{bmatrix} 1 - \frac{\sigma_i \pi l}{\lambda} \Psi_A \Psi_B & -\frac{\sigma_i \pi l \Psi_B^2}{\lambda} \\ \frac{\sigma_i \pi l \Psi_A^2}{\lambda} & 1 + \frac{\sigma_i \pi l}{\lambda} \Psi_A \Psi_B \end{bmatrix} \begin{bmatrix} a_i \\ b_i \end{bmatrix} \tag{11}$$

where we have used the Wronskian $\mathcal{W}\left[\Psi_A(x), \Psi_B(x)\right] = -\frac{\lambda}{l\pi}$. Inserting Ψ_A and Ψ_B, Equation (11) becomes

$$\begin{bmatrix} a_{i+1} \\ b_{i+1} \end{bmatrix} = \mathbb{M}_i \begin{bmatrix} a_i \\ b_i \end{bmatrix} \tag{12}$$

where the transfer matrices $\mathbb{M}_i$ are given as

$$\mathbb{M}_i = \begin{bmatrix} 1 - \frac{\sigma_i \pi l Ai(u_i)[Ai(u_i) - \lambda Bi(u_i)]}{\lambda} & -\frac{\sigma_i \pi l}{\lambda} \left[Ai(u_i) - \lambda Bi(u_i)\right]^2 \\ \frac{\sigma_i \pi l}{\lambda} Ai^2(u_i) & 1 + \frac{\sigma_i \pi l Ai(u_i)[Ai(u_i) - \lambda Bi(u_i)]}{\lambda} \end{bmatrix} \tag{13}$$

in terms of the $Ai(u)$ and $Bi(u)$. Using these transfer matrices for a finite number of Dirac delta functions, we connect the coefficients related to the rightmost region to the coefficients of the leftmost region as

$$\begin{bmatrix} a_{P+1} \\ b_{P+1} \end{bmatrix} = \mathbb{M}_P \ldots \mathbb{M}_2 \mathbb{M}_1 \begin{bmatrix} a_1 \\ b_1 \end{bmatrix} \quad . \tag{14}$$

Defining the total transfer matrix $\mathbb{X}$ as

$$\mathbb{X} = \mathbb{M}_P \ldots \mathbb{M}_2 \mathbb{M}_1 \tag{15}$$

and noting that boundary conditions require $a_1 = 0$ and $b_{P+1} = 0$, we obtain the equation

$$\begin{bmatrix} a_{P+1} \\ 0 \end{bmatrix} = \mathbb{X} \begin{bmatrix} 0 \\ b_1 \end{bmatrix} = \begin{bmatrix} x_{11} & x_{12} \\ x_{21} & x_{22} \end{bmatrix} \begin{bmatrix} 0 \\ b_1 \end{bmatrix} \tag{16}$$

for bound state solutions. This equation can be satisfied if and only if

$$x_{22}\left(k^2\right)=0 \tag{17}$$

which in turn yields the bound state energy spectrum of the system by using the roots k^2 of x_{22}. It is instructive to obtain the energy spectrum equation for the P=1 case in order to observe how the energy eigenvalues change as the dimensionless parameter (σl) varies. Since we have derived the energy equation for the general case, it is now easy to obtain it for P=1 where the total transfer matrix reduces to $\mathbb{M}_1$. By equating the x_{22} element of this matrix to zero, we obtain the desired eigenvalue equation

$$\sigma l=\frac{Ai\left(-k^2l^2\right)}{\pi Ai\left(u_1\right)\left[Ai\left(-k^2l^2\right)Bi\left(u_1\right)-Bi\left(-k^2l^2\right)Ai\left(u_1\right)\right]} \tag{18}$$

using $\lambda=\frac{Ai\left(-k^2\,l^2\right)}{Bi\left(-k^2\,l^2\right)}$ and $u_1=\frac{x_1}{l}-k^2l^2$. Note that Equation (18) reduces to the well-known energy eigenvalue equation of the linear potential

$$Ai\left(-k^2l^2\right)=0 \tag{19}$$

as $\sigma\to 0$. For different x_1 values ($x_1=0.2l,\ l,\ 5l$), we solve Equation (18) numerically for $\frac{2ml^2}{\hbar^2}E_g$ where E_g is the ground state energy and observe that E_g is a monotonically decreasing function of σl as shown in Figure (1). We also show how the ground state energy changes with the position of Dirac delta function for $\sigma l=2$ in Figure (2). ΔE_g is negative since we have used an attractive Dirac delta interaction. For very small and very large x_1 values, ΔE_g will go to zero due to the boundary conditions. By using first order perturbation theory, it can be shown that $\Delta E_n\ \propto\left|Ai\left(\frac{x_1}{l}-r_n\right)\right|^2$, where $(-r_n)$ is the n^{th} root of Ai. However, there will be two minima of ΔE_2 for the first excited state which has a node and also becomes zero at the boundaries. Figure (3) shows the graph of ΔE_2 as a function of the position x_1 of the Dirac delta function. ΔE_2 is zero at the node of the first excited state wavefunction. In general, the change in energy levels as a function of the positions of Dirac delta functions will be a complicated function since there will be several extremum points of $|\Psi_n|^2$ for excited states, $n\geq 2$.

For $P>1$, the energy spectrum can be found by using equation (17). However, the x_{22} element of the total transfer matrix becomes more complicated for these cases. For investigating the effects of attractive (A) and repulsive (R) Dirac delta potentials at $x_1=l,\ldots,x_P=Pl$ on energy levels, we solve Equation (17) for the P=1, 2, 4, 8 cases with several different configurations. For demonstrating all these results together in a figure, we define configuration numbers for different ordered configurations presented in Table 1. For example, for P=4, the four ordered Dirac delta functions shown as $AAAA$ or A^4 has the configuration number 1, and $ARRA$ or AR^2A has the configuration number 7 (which has successive A, R, R, A Dirac delta functions at points x_1, x_2, x_3, x_4 where $x_1<x_2<x_3<x_4$). We choose configuration numbers such that configurations with more repulsive Dirac delta functions at smaller x_i values have higher configuration numbers.

The ground state energy as a function of these configuration numbers is presented in Figures (4-A) and (4-B) with strengths $\sigma=|\frac{1}{l}|$ and $\sigma=|\frac{5}{l}|$ respectively ($\sigma=\frac{1}{l},\frac{5}{l}$ and

N_{conf}	P=1	P=2	P=4	P=8
1	A	A^2	A^4	A^8
2	R	AR	A^3R	A^4R^4
3	-	RA	A^2RA	R^4A^4
4	-	R^2	A^2R^2	R^8
5	-	–	ARA^2	–
6	-	–	$ARAR$	–
7	-	–	AR^2A	–
8	-	–	AR^3	–
9	-	–	RA^3	–
10	-	–	RA^2R	–
11	-	–	$RARA$	–
12	-	–	RAR^2	–
13	-	–	R^2A^2	–
14	-	–	R^2AR	–
15	-	–	R^3A	–
16	-	–	R^4	–

Table 1 Configuration Numbers (N_{conf}) for ordered P=1, 2, 4, 8 Dirac delta functions. A and R denote attractive and repulsive Dirac delta functions respectively.

$\sigma = -\frac{1}{l}, -\frac{5}{l}$ for attractive (A) and repulsive (R) delta functions respectively). We notice that for the same $|\sigma|$ value, the attractive Dirac delta functions decrease the energy (E_g) value more than the repulsive Dirac delta functions increase it. For example, compare the A^4 and R^4 cases with zero delta function values in Figures (4) and (5). This can also be seen in Figure (1) for the P=1 case. One can qualitatively explain this effect by considering the change of the wave function. The wave function should have a kink at $x = x_i$ with a finite jump for derivatives at $x = x_i - \epsilon$ and $x = x_i + \epsilon$ in order to satisfy $\frac{d\Psi}{dx}|_{x=x_i+\epsilon} - \frac{d\Psi}{dx}|_{x=x_i-\epsilon} = -\sigma\Psi$. Thus, the wavefunction forms an outward kink and increases the value of $|\Psi|^2$ for attractive Dirac delta potential, and forms an inward kink and decreases the value of $|\Psi|^2$ for repulsive Dirac delta potential. Thus, the attractive Dirac delta functions will cause much bigger changes in energy E_n since the energy change due to Dirac delta functions, ΔE_n, is proportional to $|\Psi_n|^2$.

In order to show how the energy levels of a charged particle change in case of one impurity located at $x = l$, in Table 2 we have investigated the change in the bound state energy levels where one Dirac delta function is added to the linear potential. We have exhibited E_n in units of $\frac{\hbar^2}{2ml^2}$ for attractive ($\sigma l = 2$) and repulsive ($\sigma l = -2$) cases. The change in the ground state energy is the largest. As we have discussed above, this is due to the value of $|\Psi_n|^2$ at the position of the Dirac function $x_1 = l$.

Finally we investigated the change in ground state energy for 8 Dirac delta functions at random locations between 0 and 10 l. By using the given electric field $E_s = 7.5\,10^4\,V/cm$ and the effective mass of an electron $m^* = 0.067\,m_0$ for GaAs/GaAlAs heterostructure [14, 15], we estimate the parameter l given in Equation (4) as 42 Å. This result shows

n	E(DDLP) $\sigma l = 2$	E(DDLP) $\sigma l = -2$	E(LP)
1	0.568	2.923	2.338
2	3.717	4.554	4.088
3	5.347	5.829	5.521
4	6.704	6.941	6.787
5	7.909	8.000	7.944
6	9.012	9.036	9.023
7	10.040	10.041	10.040
8	11.007	11.006	11.009
9	11.925	11.945	11.936
10	12.803	12.847	12.829

Table 2 The energies E_n (in units of $\frac{\hbar^2}{2ml^2}$) for the low-lying bound states (n=1-10) with linear potential (LP) and delta decorated linear potential (DDLP) which contains one Dirac delta functions at $x_1 = l$. $\sigma l = +2$ and $\sigma l = -2$ represent attractive and repulsive Dirac delta potentials respectively.

that there exists, on average, one impurity per 50 Å along a one-dimensional wire, which is a realistic choice. We have studied four cases:

a) **Attractive impurities**: All the Dirac delta functions are attractive with strengths $\sigma_i l = 2$,

b) **Repulsive impurities**: All the Dirac delta functions are repulsive with strengths $\sigma_i l = -2$,

c) **Mixed aR-Type impurities**: The strengths of the Dirac delta functions are also determined randomly, as either $\sigma_i l = 1$ or $\sigma_i l = -2$,

d) **Mixed Ar-Type impurities**: Same as in part c) but randomly chosen strengths are with $\sigma_i l = 2$ or $\sigma_i l = -1$.

Cases a) and b) represent the model of one type (attractive or repulsive) of impurities in a system. Case c) and d) are for models of different type impurities in a system. For Case c), repulsive impurities have the strengths twice the strength of attractive ones. For Case d), it is the opposite. By performing these calculations, we have investigated the effects of locations, types and strengths of impurities on the ground state energy. We have done 1000 calculations for each cases. The number of ground states versus ground state energy (E_g) is plotted in Figures (6–9) for Cases a)–d). The intervals are chosen as the 0.1 unit on the x-axis to obtain box diagrams. Since the locations are chosen randomly, E_g can have values in a wide range of energies. For these 1000 calculations, the average (E_{av}) and the maximum occurring energy (E_{peak}) are obtained and shown in Table 3. Comparisons of the ground state energy $E_g = 2.338$ of the linear potential with E_{av} values for these four cases again demonstrate that the attractive interactions are more effective than repulsive interactions.

Triangular quantum well structures have been studied to explain the electronic properties of semiconductor heterostructures. For a GaAs/GaAlAs semiconductor, charge

	Attractive $\sigma l = 2$	Repulsive $\sigma l = -2$	Attractive($\sigma l = 1$) Repulsive($\sigma l = -2$)	Attractive($\sigma l = 2$) Repulsive($\sigma l = -1$)
E_{peak}	-0.4	3.4	2.3	0.9
E_{av}	-1.061	3.322	1.886	1.095

Table 3 Energies (in units of $\frac{\hbar^2}{2ml^2}$) which are obtained by performing 1000 calculations with attractive and repulsive Dirac delta functions at random locations. (See Figures (6–9) and text.)

transfers create an electric field at the junction of GaAs and GaAlAs. This electric field can be taken as approximately constant [14]. Thus, we obtain a linear potential due to this constant electric field. If there exist impurities in this system, then the effects of impurities should be added to this linear potential. In our paper, we investigate these effects by using Dirac delta functions which can model very short-range impurity potentials. As we mentioned above, this one-dimensional model can be used to describe the bound state energy levels of a charged particle which moves in a constant electric field ($\overrightarrow{E} = -E_0\hat{x}$) on the positive half-line with impurities at $x = x_i$ and impenetrable boundary at x=0. The linear potential due to the constant electric field will shift the Fermi level of this heterostructure by the amount of the ground state energy of the linear potential [14]. Thus, the ground state energy for the linear potential and hence the Fermi energy of the system change by adding impurities. By using the calculated $l = 42$ Å for GaAs/GaAlAs and Dirac Delta interaction with strength $\sigma = \frac{2}{42}\frac{1}{\text{Å}}$ ($\sigma = -\frac{2}{42}\frac{1}{\text{Å}}$), we find that the Fermi energy decreases by $56\,meV$ (rises by $19\,meV$) for an attractive (repulsive) Dirac delta function located at $x_1 = l$ (Table 2).

Until this point, we have assumed $Bi\left(-k^2\,l^2\right) \neq 0$. However, as σ varies, the solution of Equation (18) may yield k values that satisfy

$$Bi\left(-k^2\,l^2\right) = 0 \ . \tag{20}$$

In this case, the $Bi\left(u\right)$ part of the wave function in Equation (7) satisfies the boundary condition at $x = 0$. Then, for this specific value of k, only the wavefunction of the first interval should be modified as

$$\Psi_1 = b_1\Psi_B\left(u\right) = b_1 Bi\left(u\right) \ . \tag{21}$$

The wavefunctions for all intervals except $i = 1$ preserve their forms as given in Equations (8) and (9). Note that for the $Bi\left(-k^2l^2\right) = 0$ case, Equation (18) for P=1 reduces to

$$\sigma l = \frac{1}{\pi Ai\left(\frac{x_1}{l} - k^2l^2\right)\ Bi\left(\frac{x_1}{l} - k^2l^2\right)} \ . \tag{22}$$

By using $\Psi\left(r\right) = \frac{F(r)}{r}$ for the radial function, the above calculations may also be used to find the exact s state solutions ($L = 0$) of the three-dimensional Schrödinger equation with linear potential.

3 Conclusion

In this paper, we have studied bound states of the Schrödinger equation with Dirac delta decorated linear potential. The potential is given as

$$V(x) = f\,x - \frac{\hbar^2}{2m}\sum_{i=1}^{P}\sigma_i\,\delta(x - x_i) \quad .$$

We have obtained transfer matrices and the eigenvalue equation by using the x_{22} element of the total transfer matrix $\mathbb{X}$. We have presented the wavefunctions in terms of Airy functions Ai and Bi. For P=1, we have obtained a transcendental equation for the bound state energies and calculated the change of energies for the low-lying bound states (n=1–10) for a linear potential with attractive or repulsive Dirac delta functions. We have used these results to calculate the shift of the Fermi energy of electron gas in a GaAs/GaAlAs junction containing an impurity.

By solving the eigenvalue equation for P=1, 2, 4, 8, we have investigated the change in the ground and first excited state energies for different strengths and positions of Dirac delta functions. We have also investigated the change in the ground state energy for a linear potential with Dirac delta functions at random locations.

Our calculations may also be used to solve exactly s state ($L = 0$) solutions of the three-dimensional Schrödinger equation with linear potentials by making a suitable change of variable in the radial part of the wavefunction.

Our methodology can also be useful for some other physical systems with potential containing contact (point) interactions.

Acknowledgment

This work has been supported by the Turkish Academy of Sciences, in the framework of the Young Scientist Award Program (ED- TÜBA- GEBIP- 2001-1-4), BU Research Funds, grant number 04HB301.

References

[1] W. Greiner and B. Müller: *Quantum Mechanics: Symmetries*, 2nd revised Ed., Springer-Verlag, Berlin, 1994.

[2] B. Govoreanu , P. Blomme, M. Rosmeulen, V.J. Houdt and K. De Meyer: "A model for tunneling current in multi-layer tunnel dielectrics" *Solid State Electronic*, Vol. 47, (2003), pp. 1045–1053.

[3] P. Fendley: "Airy Functions in Thermodynamics Bethe Ansatz" *Lett.Math.Phys.*, Vol. 49 , (1999), pp. 229–233.

[4] J.Z. Imbrie: "Dimensional reduction and crossover to mean-field behavior for branched polymers" *Ann. Henri Poincare*, Vol. 4, (2003), pp. 445–458.

[5] S. Flügge: *Practical Quantum Mechanics*, Springer, New York, 1974.

[6] S. Alveberio, F. Gesztsy, P. Høegh-Krohn and H. Holden: *Solvable Models in Quantum Mechanics*, Springer, New York, 1988.

[7] E. Demiralp and H. Beker: "Properties of bound states of the Schrödinger equation with attractive Dirac delta potentials", *J.Phys.A: Math. Gen.*, Vol. 36, (2003), pp. 7449–7459.

[8] C. Cohen-Tannoudji, B. Diu and F. Laloë: *Quantum Mechanics I*, Hermann, Paris, 1977.

[9] C. Kittel: *Introduction to Solid State Physics*, 7th Ed., John Wiley, New York, 1996.

[10] T. Uchino and I. Tsutsui: "Supersymmetric quantum mechanics under point singularities" *J. Phys A:Math.Gen*, Vol. 36, (2003), pp. 6821–6846.

[11] J. R. Barker: "The physics and fabrication of microstructures and microdevices", In: M.S. Kelly and C. Weisbuch (Eds.): *Proceedings in Physics, 13*, Springer, New York, 1986, pp. 210–220.

[12] W. Ellberfeld and M. Kleber: *Zeitschrift für Physik B*, Vol. 73, (1988), pp. 23–32.

[13] G. Álvarez and B. Sundaram: "Perturbation theory for the Stark effect in a double δ quantum well" *J. Phys. A: Math Gen.*, Vol. 37, (2004), pp. 9735–9748 .

[14] C. Weisbuch and B. Vinter: *Quantum Semiconductor Structures:fundamentals and Applications*, Academic Press, San Diego, 1991.

[15] S.B. Monozon, V.M. Ivanov and P. Schmelcher: "Impurity center in a semiconductor quantum ring in the presence of a radial electric field", *Physical Review B*, Vol. 70, (2004), pp. 205336–205347.

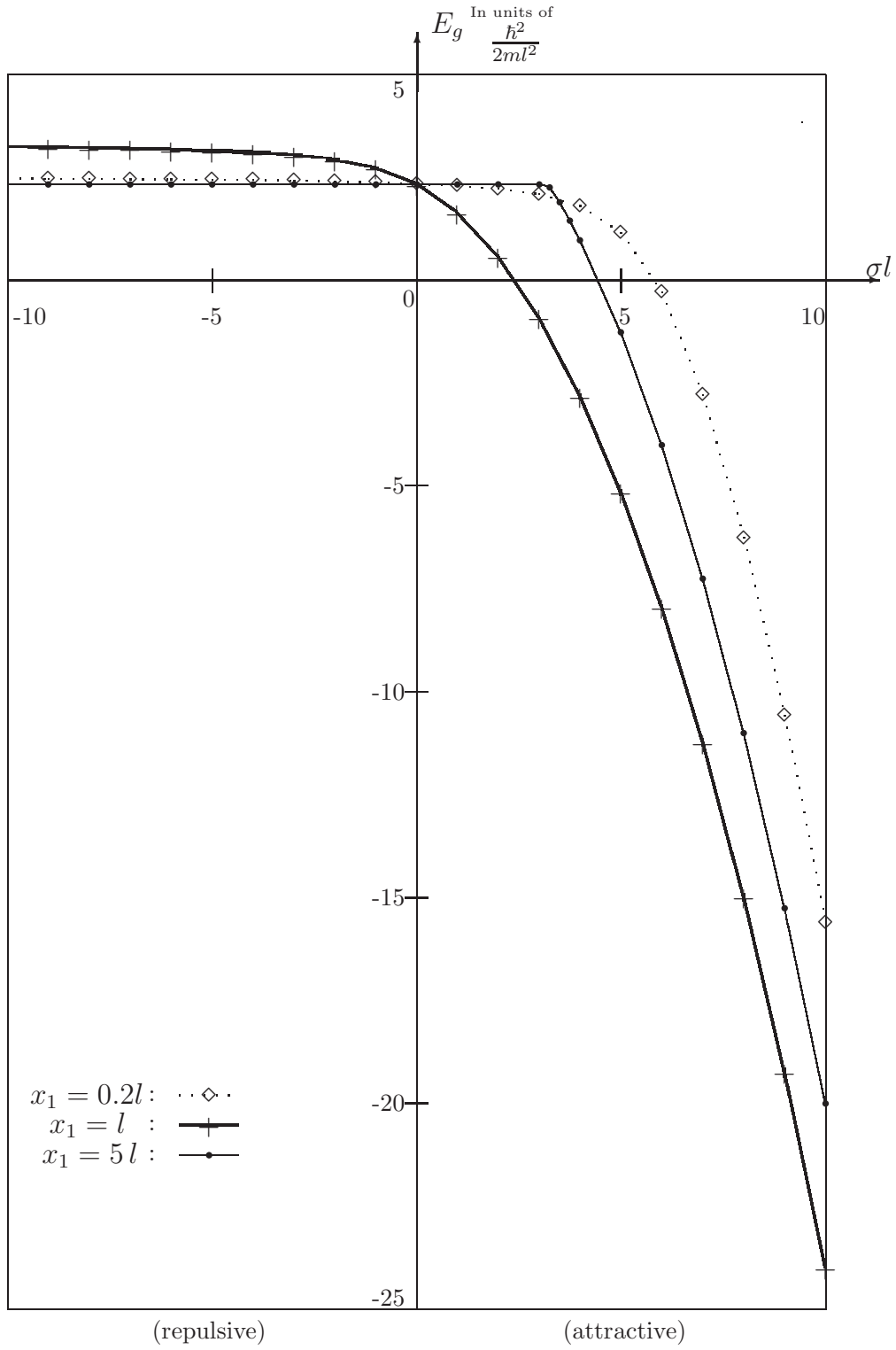


Fig. 1 The energies (E_g) (in units of $\frac{\hbar^2}{2ml^2}$) vs. (σl), where E_g is the ground state energy.

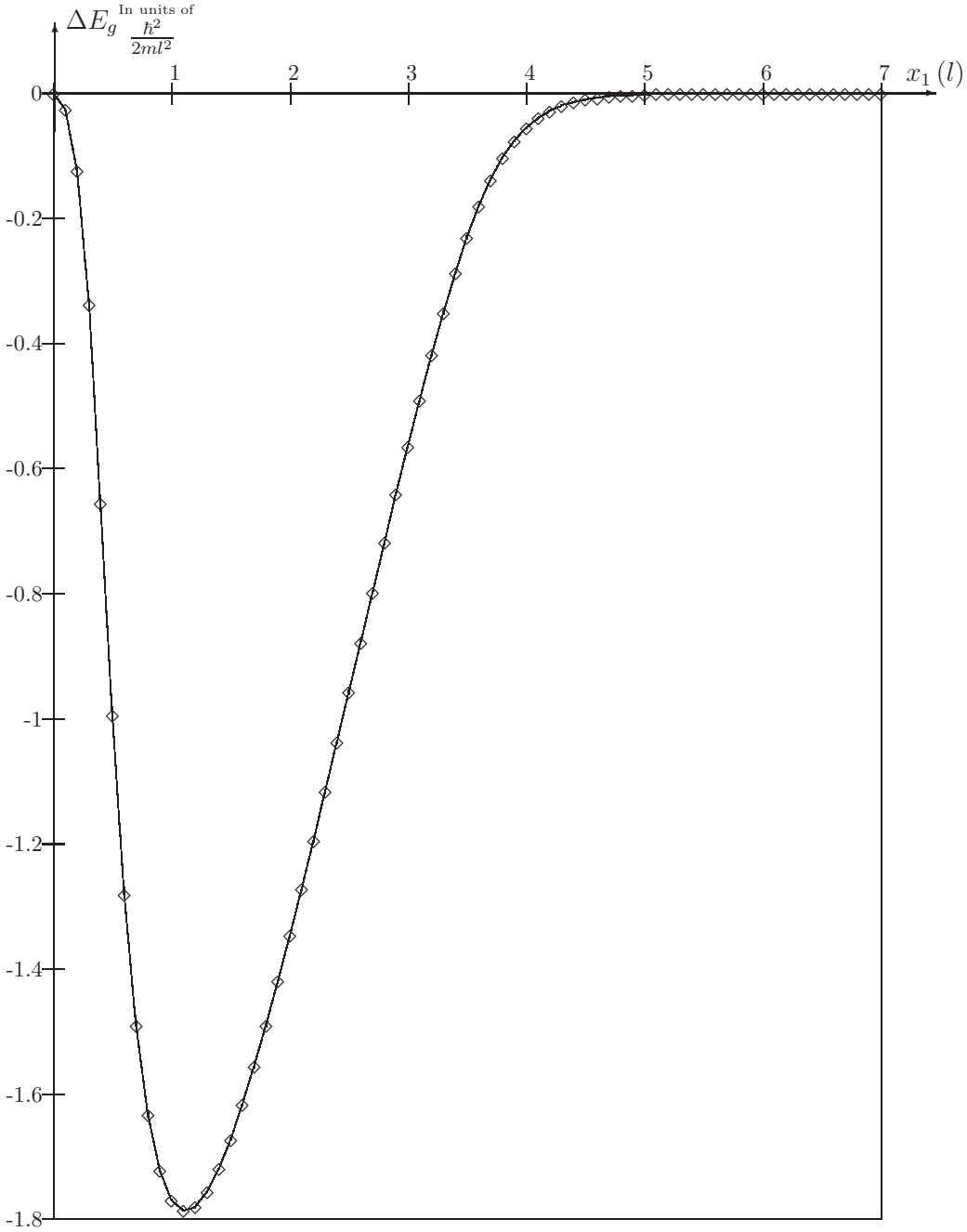


Fig. 2 The change of ground state energy (ΔE_g) (in units of $\frac{\hbar^2}{2ml^2}$) vs. the position of the Dirac delta function x_1 for $\sigma l = 2$. x_1 is in units of l.

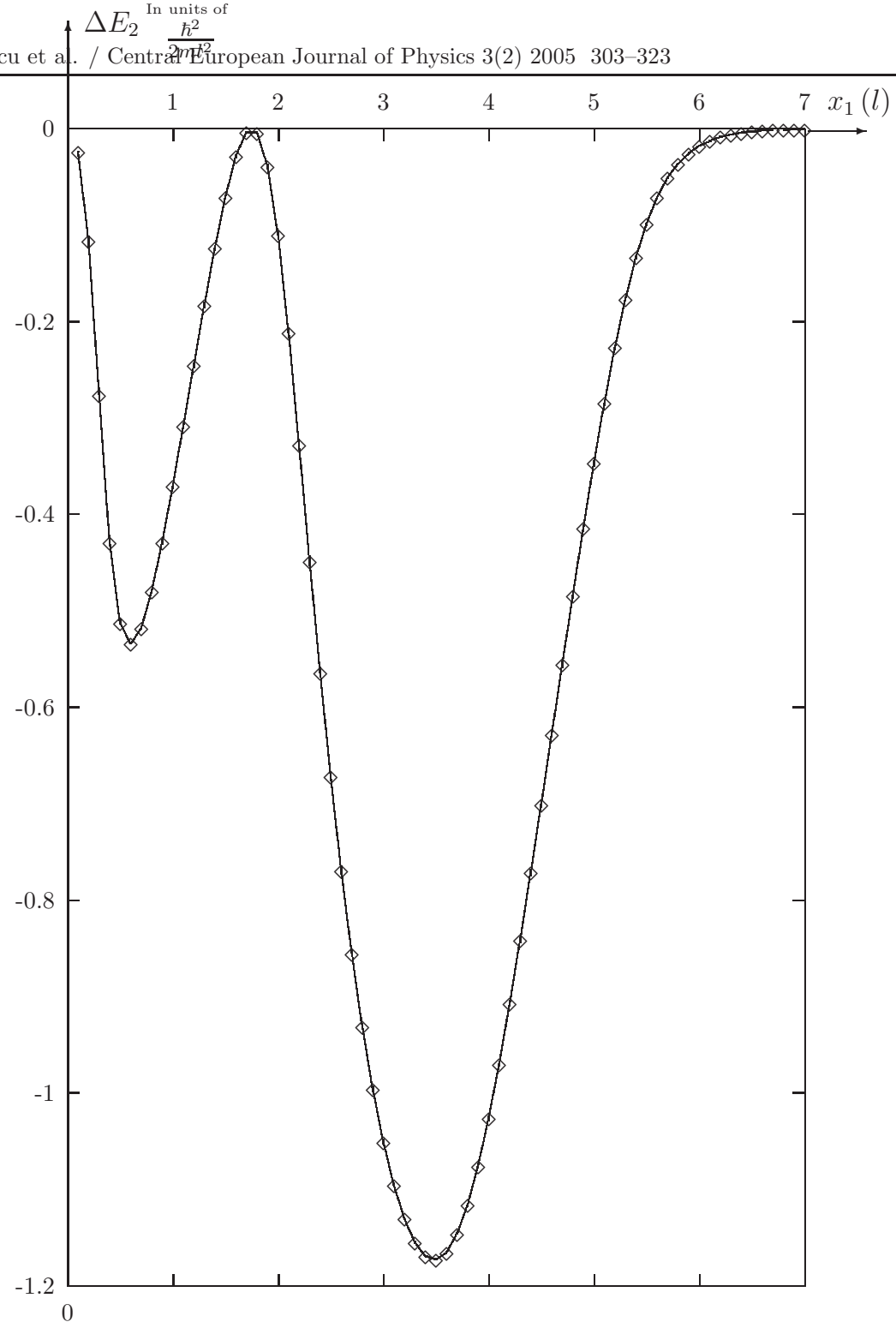


Fig. 3 The change of energy in the first excited state (ΔE_2) (in units of $\frac{\hbar^2}{2ml^2}$) vs. the position of the Dirac delta function x_1 for $\sigma l = 2$, where E_2 is the first excited state. x_1 is in units of l.

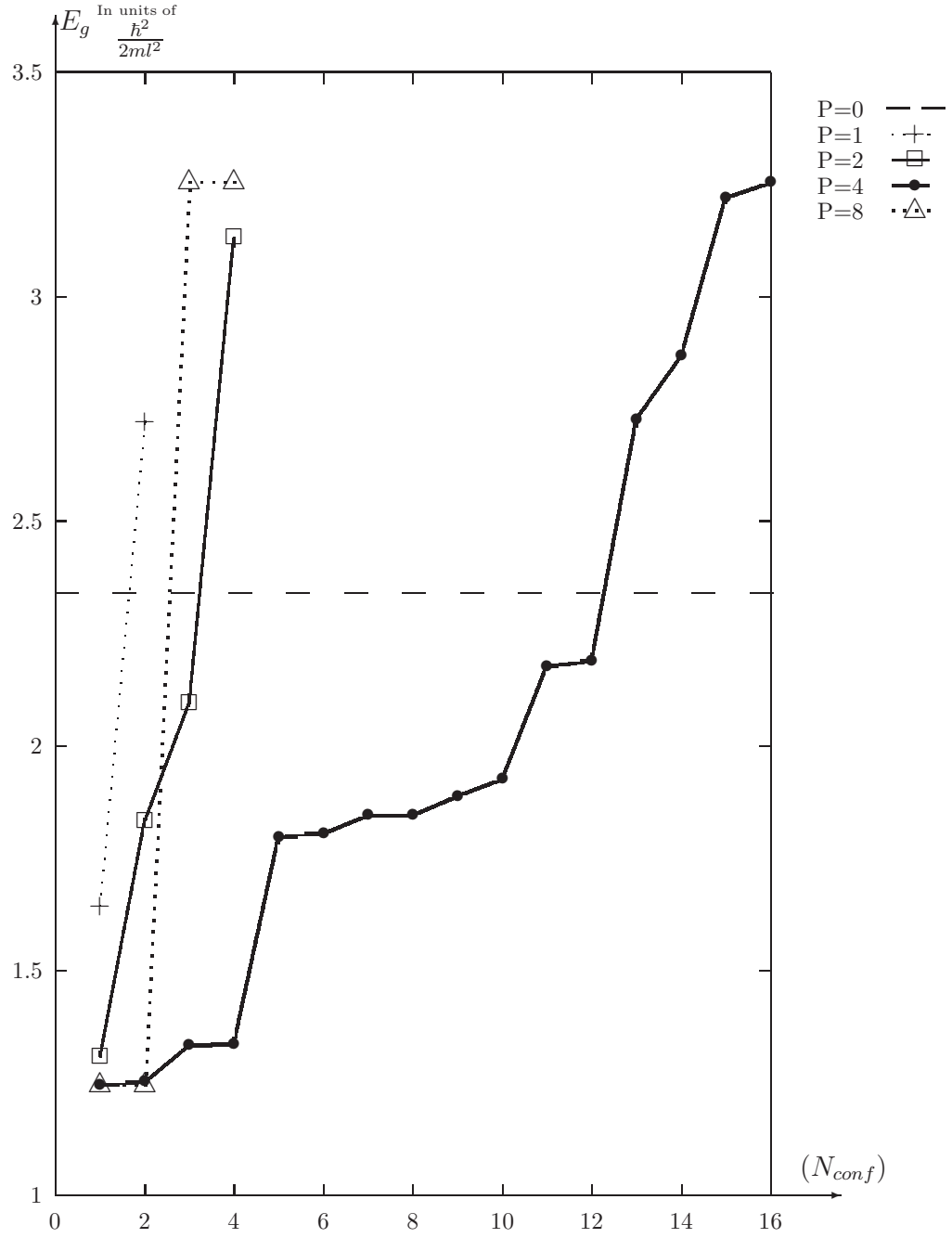


Fig. 4-A The ground state energy E_g (in units of $\frac{\hbar^2}{2ml^2}$) vs. configuration number (N_{conf}) of different arrangements (see Table 1) of Dirac delta functions at $x_1 = l, \ldots, x_P = Pl$ for $|\sigma|l = 1$. Lines are drawn to guide the eye.

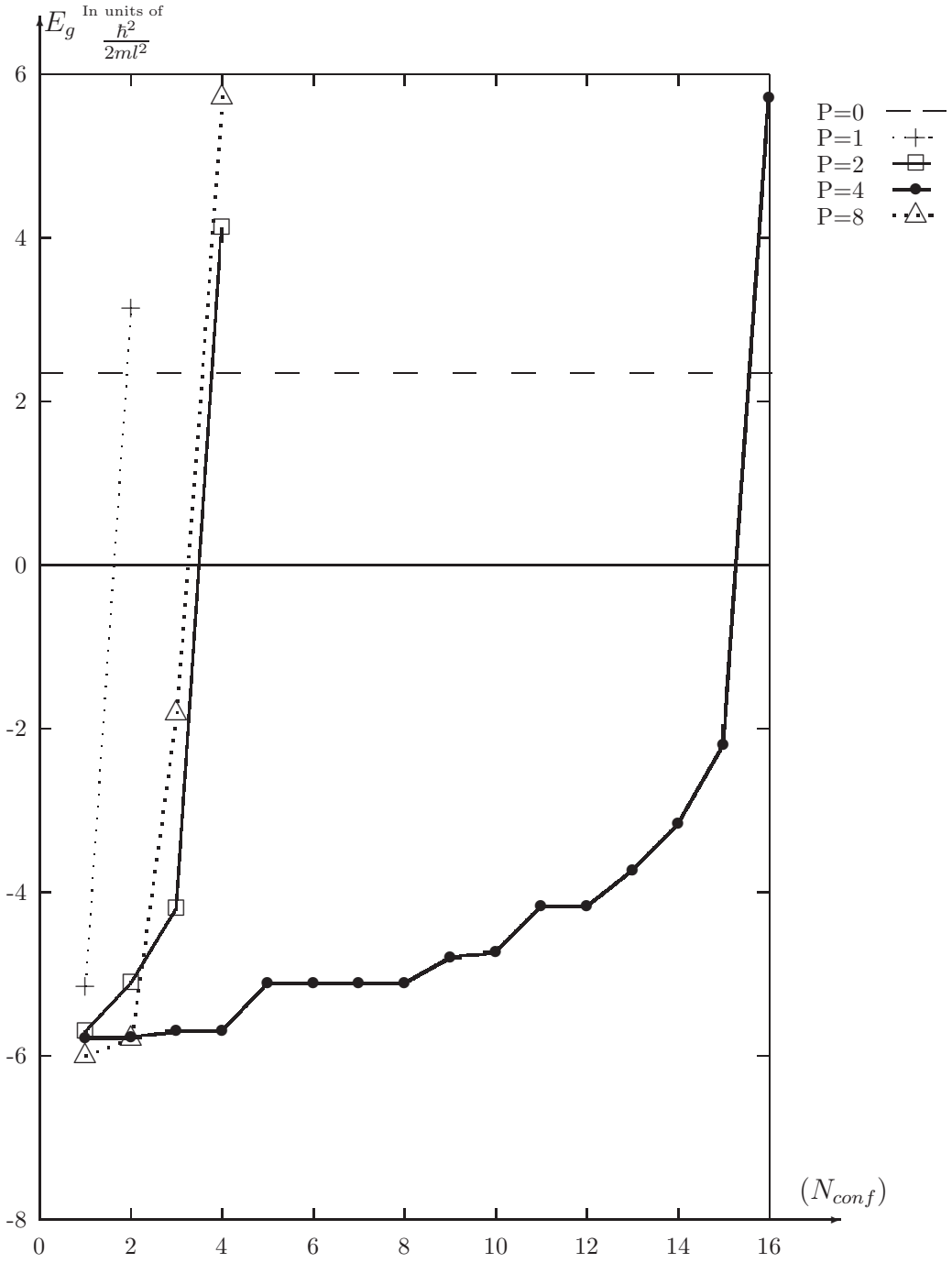


Fig. 4-B The ground state energy E_g (in units of $\frac{\hbar^2}{2ml^2}$) vs. configuration number (N_{conf}) of different arrangements (see Table 1) of Dirac delta functions at $x_1 = l\,, \ldots\,, x_P = Pl$ for $|\sigma|l = 5$. Lines are drawn to guide the eye.

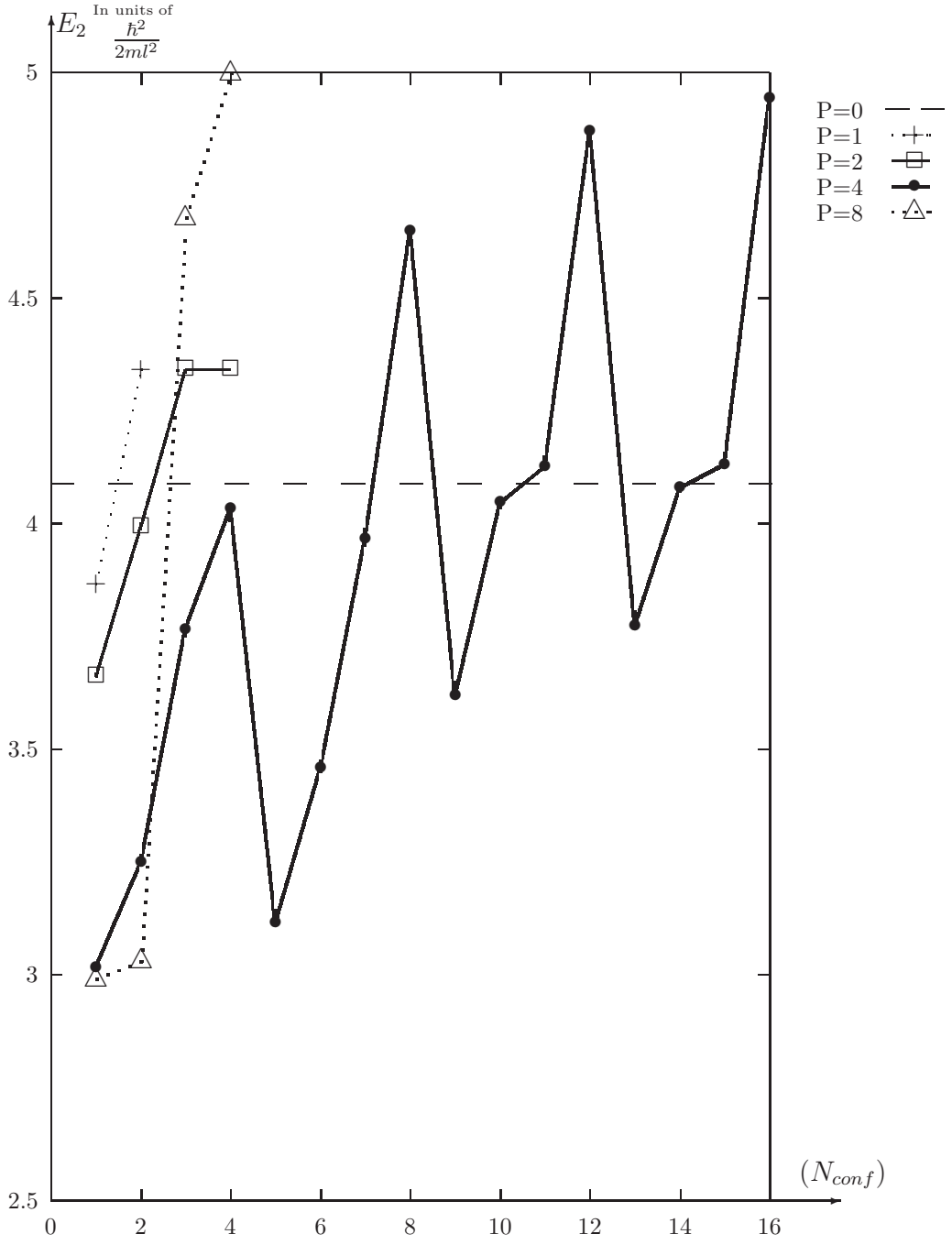


Fig. 5-A The first excited state E_2 (in units of $\frac{\hbar^2}{2ml^2}$) vs. configuration number (N_{conf}) of different arrangements (see Table 1) of Dirac delta functions at $x_1 = l\,, \ldots\,, x_P = Pl$ for $|\sigma|l = 1$. Lines are drawn to guide the eye.

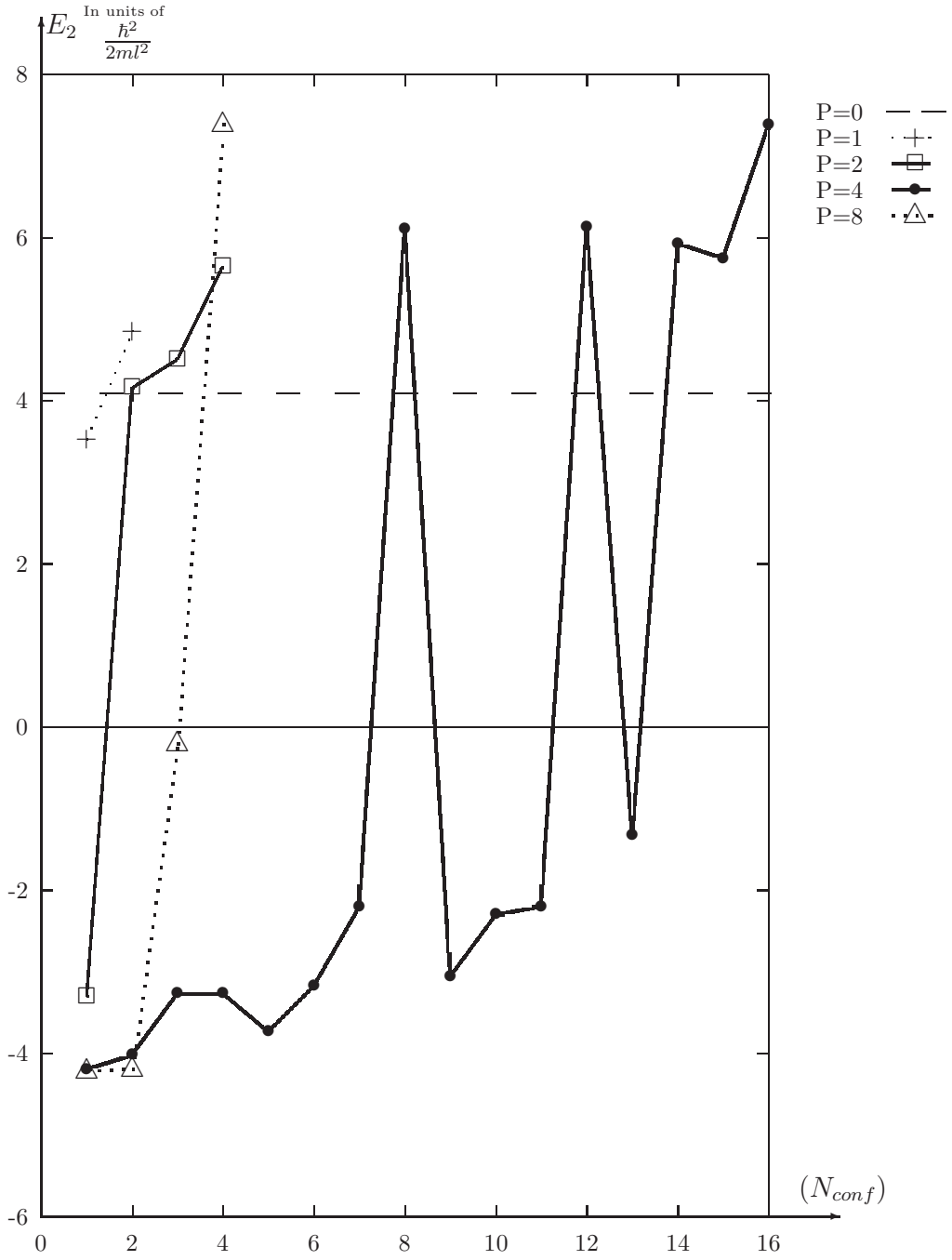


Fig. 5-B The first excited state E_2 (in units of $\frac{\hbar^2}{2ml^2}$) vs. configuration number (N_{conf}) of different arrangements (see Table 1) of Dirac delta functions at $x_1 = l\,, \ldots\,, x_P = Pl$ for $|\sigma|l = 5$. Lines are drawn to guide the eye.

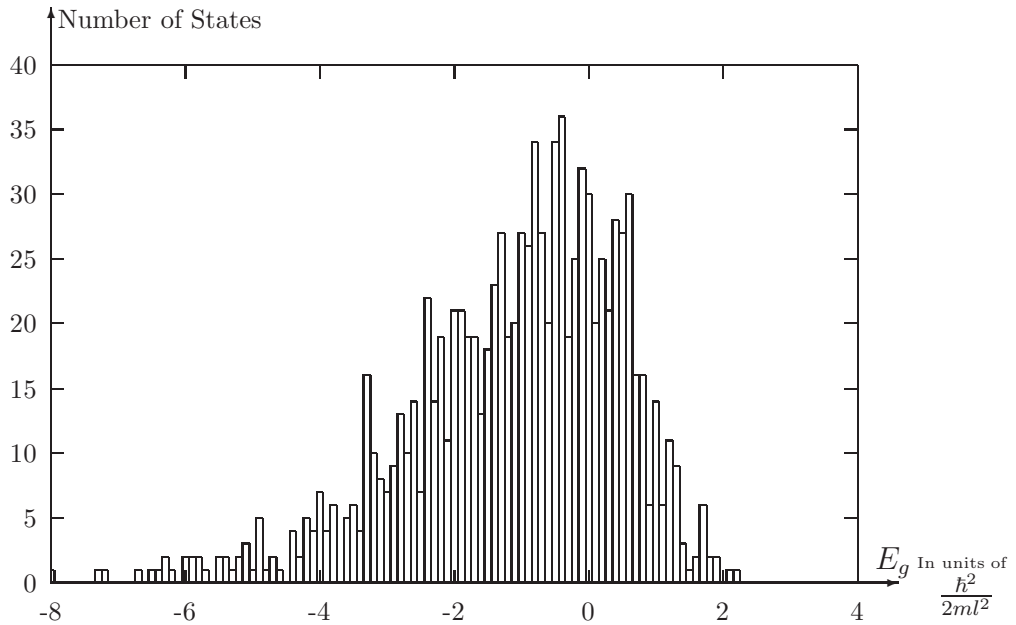


Fig. 6 Number of states in an interval (0.1 unit) (box diagram) vs. ground state energy E_g (in units of $\frac{\hbar^2}{2ml^2}$) for 1000 calculations with 8 attractive Dirac delta functions at random locations.

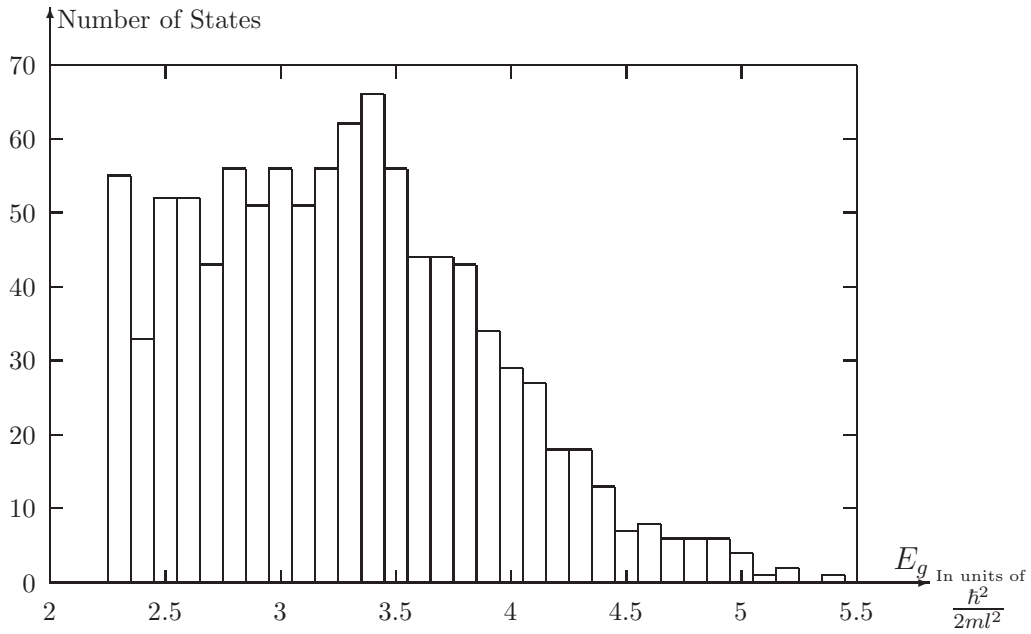


Fig. 7 Number of states in an interval (0.1 unit) (box diagram) vs. ground state energy E_g (in units of $\frac{\hbar^2}{2ml^2}$) for 1000 calculations with 8 repulsive Dirac delta functions at random locations.

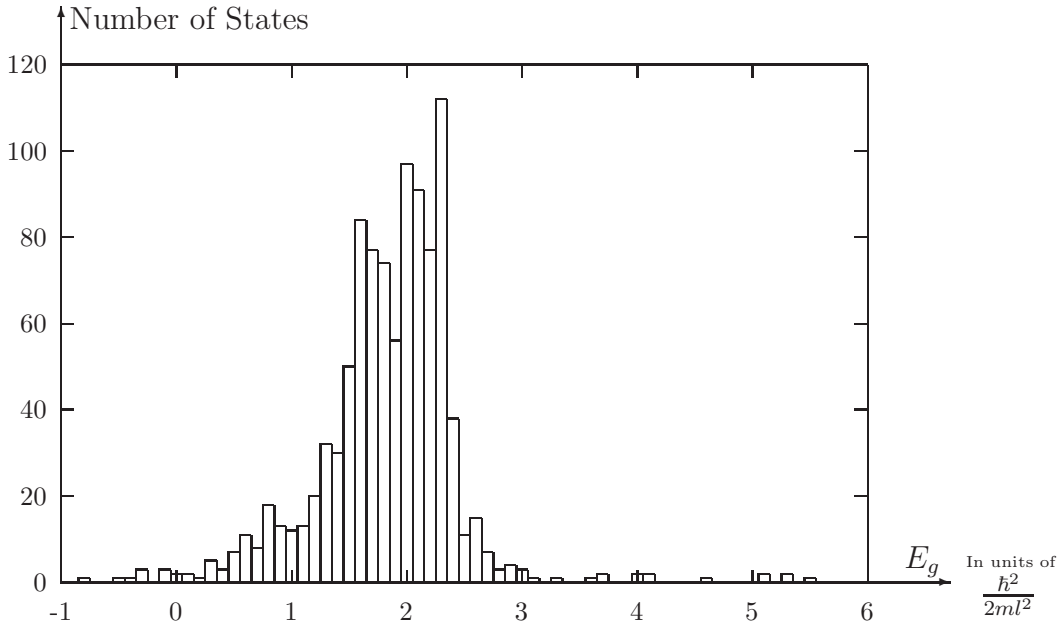


Fig. 8 Number of states in an interval (0.1 unit) (box diagram) vs. ground state energy E_g (in units of $\frac{\hbar^2}{2ml^2}$) for 1000 calculations with 8 Dirac delta functions at random locations with different strengths ($\sigma_{att}l = 1$, $\sigma_{rep}l = -2$). See text for explanation for the choice of strengths.

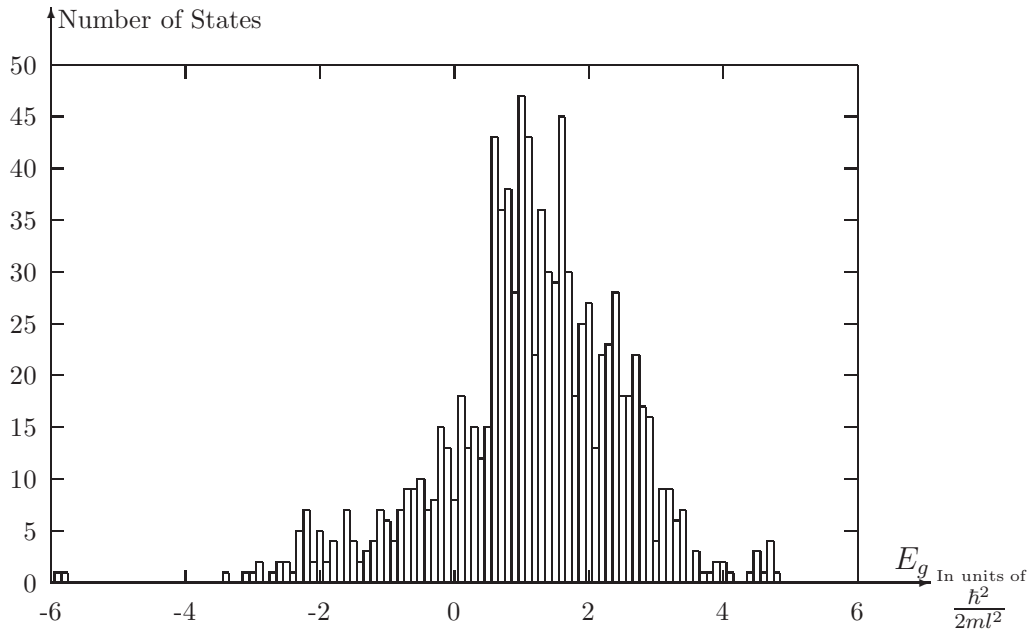


Fig. 9 Number of states in an interval (0.1 unit) (box diagram) vs. ground state energy E_g (in units of $\frac{\hbar^2}{2ml^2}$) for 1000 calculations with 8 Dirac delta functions at random locations with different strengths ($\sigma_{att}l = 2\,,\ \sigma_{rep}l = -1$). See text for explanation for the choice of strengths.